Sensor and Simulation Notes

Note 571

12 September 2015

Considerations for a Compact Loop Antenna and the Benefits of Subdividing the Loop into many Loops

D. V. Giri

Pro-Tech, 11-C Orchard Court, Alamo, CA 94507-1541
Dept. of Electrical and Computer Engineering, Univ. of New Mexico, Albuquerque, NM 87131

and

F. M. Tesche
1519 Miller Mountain Road, Saluda, NC 28773

Abstract

This note deals with the design considerations of a magnetic dipole antenna driven by a compact Marx source. Given the capacitive source, the antenna provides an inductive load to the source thus, creating a resonant circuit that radiates with a certain amount of magnetic moment. This LC-type of resonance is in addition to the loop resonance and occurs at a frequency lower than the loop resonance. Various design parameters and their effect on the resonant frequency and the radiation patterns are studied in this report to aid in the actual fabrication and testing. We have looked at dividing a single loop into N sub-loops and find that the loop inductance goes down by a factor of N, the resonant frequency goes up by a factor of N and the radiated field goes up by a factor of N^2.Subdividing the loop is seen to have definite advantages.

This work was sponsored by Air Force Research Laboratory/ DEHP, Kirtland AFB, NM 87117 under their Ultra Wideband Sources and Antenna (USA) Program, Govt. Contract Number: F29601-00-D-0074 in 2005.

1. Introduction

An example of a compact source/antenna system is the DIEHL 110 (see Figure 1) offered commercially by Diehl, Munitionssysteme GmbH & Co in Germany [1].

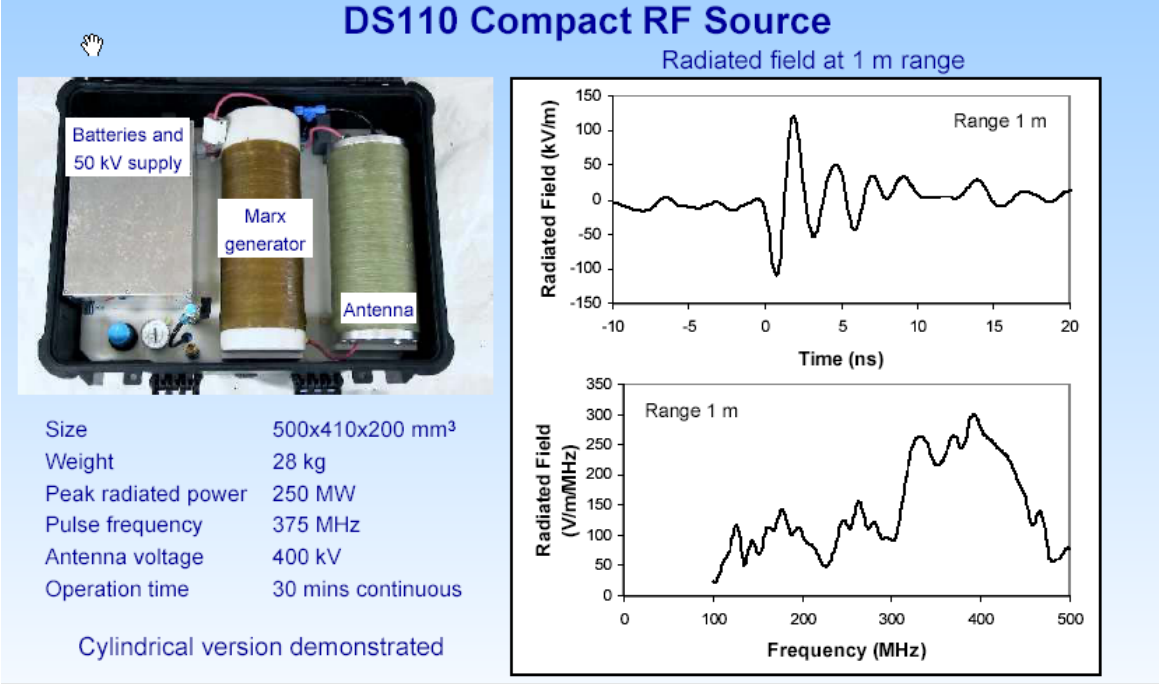

Figure 1. DIEHL 110 Compact source and the electric field at 1m

We observe that the main radiation frequency is ~ 375 MHz or a wavelength λ of 80 cm. Using the far field criteria of (kr~1) and r > antenna size, it is observed that the 1m range is already in the far field. The measured positive peak of 125 kV/m at a range of 1m in the far field gives an (r E_p) of 125 kV and an (r E_p/V) = 125 kV/400 kV = 0.3125. The dimension of the system along the axis of the antenna, which is also parallel to the axis of the Marx cylinder, is 41 cm. The antenna is likely to be a half-wave electrical dipole with a total length of ~ 40 cm = $(\lambda/2)$ and the resulting frequency is 375 MHz, which is what is advertised. There are two skinny wires (red in color) entering the antenna cylinder from the two ends. It is likely that these two wires activate a switch at the center of the dipole. The skinny wires would have excessive inductance to result in a 375 MHz, LC type of resonance.

Given the above background, we now consider a given set of maximum dimensions of length ℓ = 0.6 m, height h = 0.45 m, and width w = 0.3 m and also a capacitive source. For a capacitive source, an inductive load offered by a loop antenna (magnetic dipole) is a natural choice for creating an LC resonance that occurs below the loop resonance in the present case. It is also desirable to maximize the magnetic dipole moment of the radiator to get the highest possible field. The magnetic dipole moment is simply the loop current times the area of the loop at frequencies where the current around the loop can be regarded as a constant. In contrast, an electrical dipole driven by a capacitive source will not display the LC resonance,

but will exhibit only the half-wave dipole resonance. For these reasons we are considering a loop antenna with maximum dimensions outlined above.

2. Low Frequency Analysis of the Loop Antenna

2.1 Evaluation of the Loop Current

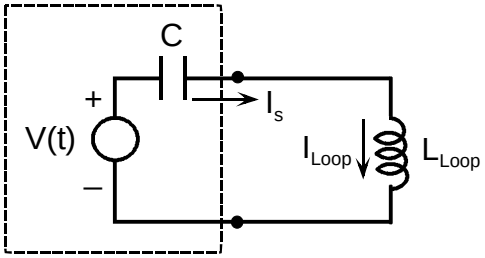

Figure 2. Simple equivalent circuit of the pulser source and radiating loop antenna

For the determination of the current flowing in the pulser circuit of Figure 2, standard circuit analysis techniques are used [2]. For a capacitor C having an initial voltage V_o switched into the circuit at time $t = t_1$, the induced current response can be calculated by considering a step function excitation voltage $V(t) = V_o\ [U(t\text{-}t_1)]$ applied to the circuit. In the frequency domain this voltage source is given as $V(s) = V_o/s$, where $s = j\omega$ and $t_1 = 0$

In the frequency domain the loop current is given by

$$I_{Loop}(s) = (V_o / s)\left(\frac{s/L}{s^2 + 1/(LC)}\right) = \left(\frac{V/L}{s^2 + \omega_o^2}\right) \tag{1}$$

where the resonance frequency $\omega_o = 1/\sqrt{LC}$, In this expression, L is the inductance of the loop.

Using the Laplace transform inversion, the transient response for the loop current in Figure 2 can be expressed analytically as

$$I_{Loop}(t) = V_o\sqrt{\frac{C}{L}}\sin\left(\omega_o(t-t_1)\right)U(t-t_1) \tag{2}$$

From this expression, we may compute the EM field produced by the circulating current.

2.2 Estimation of the Loop Inductance

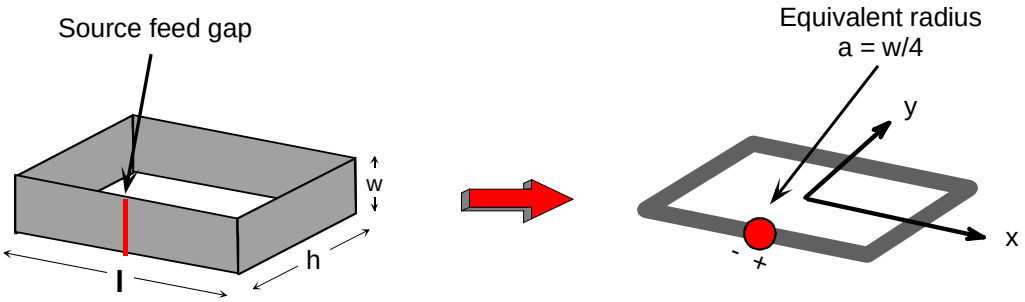

Figure 3. Equivalence of the loop antenna of width *w* and a wire loop of conductor radius *a*.

For a loop of dimensions ℓ and *h*, made of a flat plate of width *w*, there are several different equations that have been developed for computing the inductance. For the case of a thin loop, where $w << \ell$ and *h*, Grover [3] provides the following expression for the inductance L:

$$L_{Grover} = 0.4\left[h\ln\left(8\frac{h}{w}\right) + l\ln\left(8\frac{l}{w}\right) + 2\sqrt{h^2+l^2} - 1.75(h+l) - h\sinh^{-1}\left(\frac{h}{l}\right) - l\sinh^{-1}\left(\frac{l}{h}\right)\right] \quad (\mu H) \quad (3)$$

Similarly, Terman [4] provides an expression for the inductance, assuming that circular wires of radius $a = w/4$ are used to replace the plates. This expression is

$$L_{Termin} = 0.4\left[(l+h)\ln\left(2\frac{lh}{a}\right) - l\ln\left(l+\sqrt{l^2+h^2}\right) - h\ln\left(h+\sqrt{l^2+h^2}\right) + 2\sqrt{l^2+h^2} + 2a - 2(l+h)\right] \quad (\mu H) \quad (4)$$

Bashenoff [5] provides a less approximate expression for the loop inductance as

$$L_{Bashenoff} = 0.4\left[(l+h)\ln\left(\frac{lh}{a(l+h)}\right)\right] \quad (\mu H). \quad (5)$$

Another expression for the loop inductance can be found using the method of partial inductance, as described by Paul [6]. This provides the following expression:

$$L_{Paul} = 0.4\left[l\ln\left(\frac{l}{a}+\sqrt{\left(\frac{l}{a}\right)^2+1}\right) + h\ln\left(\frac{h}{a}+\sqrt{\left(\frac{h}{a}\right)^2+1}\right) - l\ln\left(\frac{l}{h}+\sqrt{\left(\frac{l}{h}\right)^2+1}\right) - h\ln\left(\frac{h}{l}+\sqrt{\left(\frac{h}{l}\right)^2+1}\right)\right] (\mu H) \quad (6)$$

$$+0.4\left[2a - (l+h) + l\left(\sqrt{\left(\frac{h}{l}\right)^2+1}\right) + h\left(\sqrt{\left(\frac{l}{h}\right)^2+1}\right) - l\left(\sqrt{\left(\frac{a}{l}\right)^2+1}\right) - h\left(\sqrt{\left(\frac{a}{h}\right)^2+1}\right)\right]$$

Finally, ref.[6] provides the standard inductance of a circular loop of radius r as

$$L_{Circle} = 0.4\pi r\left[\ln\left(8\frac{r}{a}\right) - 2\right] \quad (\mu H). \tag{7}$$

This circular loop can be compared with the rectangular loop by making the loop areas the same, as

$$r = \sqrt{\frac{lh}{\pi}}. \tag{8}$$

Table 1 presents the inductance of the loop, which is denoted as L_{Loop}.

Table 1. Inductances L_{Loop} of the loop antenna (in nH) using various formulas

Grover	Terman	Partial Inductance Method	Circular Loop	Bashenoff
589 (coefficient of 4th term = 1.75) 484 (coefficient of 4th term = 2. 0) 539 (coefficient of 4th term = 1.87)	544	542	531	517

Baum [7] has indicated that the fourth term in Grover's expression should have a constant coefficient of 2 rather than 1.75. With this revision, we find that Grover's expression gives an inductance of 484 nH. These two values from Grover's expressions of 484 nH and 589 nH provide an upper and lower bound in Grover's formula. If we use an average coefficient of 1.87 for the fourth term in Grover's expression, we end up with an inductance of 539 nH which agrees well with Terman's and Paul's expressions.

Note the Terman and partial inductance method provide comparable values for the inductance. In the calculations that follow, we use the partial inductance method results.

The resonant frequency of the circuit, and hence the frequency of the radiated EM field, is $\omega_o = 1/\sqrt{LC}$. For a fixed source capacitance, the inductance of the loop antenna should be as small as possible in order to radiate at high frequencies. However, as the radiation from the antenna is proportional to the magnetic dipole moment m (t), we must keep m large.

One way of reducing the loop antenna inductance [8] is shown in Figure 4

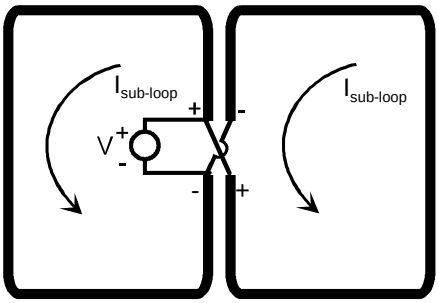

a. Subdivision into two loops

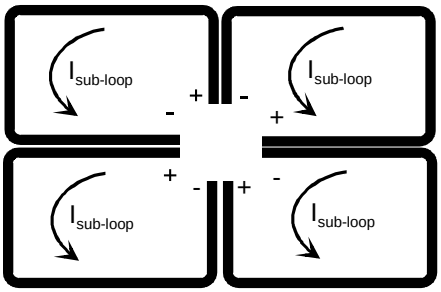

a. Subdivision into four loops

Figure 4. Subdivision of the single loop of Figure 3 into multiple loops

For the original loop divided into N sub-loops, the inductance of a single sub-loop is

$$L_{sub-loop} \approx \frac{L_{Loop}}{N} \tag{9}$$

Alternatively, the sub-loop inductance may be calculated from Eqs.(3 – 6) with modified loop dimensions.

In examining the loop interconnections in Figure 4, we note that the sub-loops are connected in parallel, as shown below. For this parallel connection, the total inductance presented to the capacitance source is

$$L_{Total} = \frac{L_{sub-loop}}{N} = \frac{L_{Loop}}{N^2} \quad \text{(approximately and not exactly)} \tag{10}$$

Thus, by subdividing the original loop into N sub-loops, the total inductance of the ensemble of loops decreases by a factor N^2, and since $\omega_o = 1/\sqrt{LC}$, the resonant frequency of the circuit will *increase* by a factor *N*.

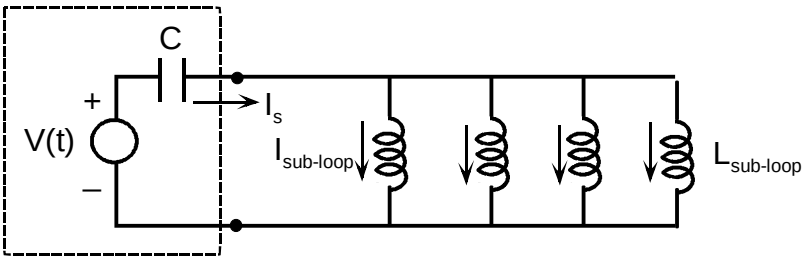

Figure 5. Equivalent circuit of a multi-loop antenna driven by the capacitive pulser

For the original loop divided into N-sub loops, the total transient source current is expressed as

$$I_s(t) = V_o N \sqrt{\frac{C}{L_{Loop}}} \sin\left(N\omega_o(t-t_1)\right)U(t-t_1) \tag{11}$$

where L_{Loop} is the original loop inductance. This source current has an amplitude N times the original source current for the single, and the factor of N higher resonant frequency is apparent in the equation. The current flowing in each sub-loop from Eq.(11) is

$$I_{sub-loop}(t) = V_o \sqrt{\frac{C}{L_{Loop}}} \sin\left(N\omega_o(t-t_1)\right)U(t-t_1)\,, \tag{12}$$

which is a current having the same amplitude at the single loop current, but with a higher oscillation frequency.

For the original loop of area $A = h\ell$, the magnetic dipole moment m is

$$\begin{aligned} m(t) &= AI_{Loop}(t) \\ &= V_o A \sqrt{\frac{C}{L_{Loop}}} \sin\left(\omega_o(t-t_1)\right)U(t-t_1) \end{aligned} \tag{13}$$

For the loop divided into N sub-loops, the dipole moment of one of the sub-loops is

$$\begin{aligned} m_N(t) &= \frac{A}{N} I_{sub-loop}(t) \\ &= V_o \frac{A}{N} \sqrt{\frac{C}{L_{Loop}}} \sin\left(N\omega_o(t-t_1)\right)U(t-t_1) \end{aligned} \tag{14}$$

And the total magnetic dipole moment is the sum of those of all of the sub-loops:

$$\begin{aligned} m_{Total}(t) &= \sum_N m_N(t) = AI_{sub-loop}(t) \\ &= V_o A \sqrt{\frac{C}{L_{Loop}}} \sin\left(N\omega_o(t-t_1)\right)U(t-t_1) \end{aligned} \tag{15}$$

Note that this equation for the divided loop dipole moment *has the same amplitude as that for the single loop* in Eq.(13), but differs by the increased frequency of oscillation. Consequently, the radiation from the four loop configuration will be different than that from the single loop, even though the dipole moments are the same.

It should also be noted that the observation that the current in each of the four sub loops is equal to the current in the single loop is valid only for frequencies near the loop resonances where the inductive reactance is about equal to the reactance of the source capacitance. At much lower frequencies, the inductive reactance is about zero and the loop currents are determined only by the source capacitance. In this case, the total currents flowing through the by the sources in the single loop and four loop cases are *equal* (given by $I = j\omega C V$), and consequently, the current in one of the four sub loops is ¼ of the single loop current.

2.3 Numerical Results

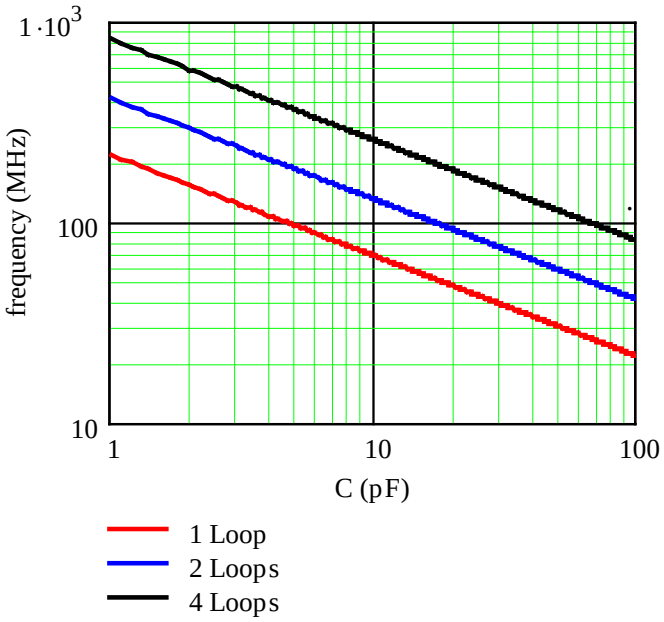

Figure 6. Resonant frequency of the pulser circuit for the loop antenna with overall dimensions ℓ = 0.6 m, h = 0.45 and w = 0.3 m, for different number of sub-loops, shown as a function of the pulser capacitance

NOTE: 1) The above results do not account for the Marx inductance.

2) The resonant frequency is provided strictly by the pulser capacitance and the effective loop inductance.

3) For the case of N=4, the inductance is about 33 nH and may be << Marx inductance. The pulser inductance may be the deciding factor in the resonance frequency rather than the loop inductance!

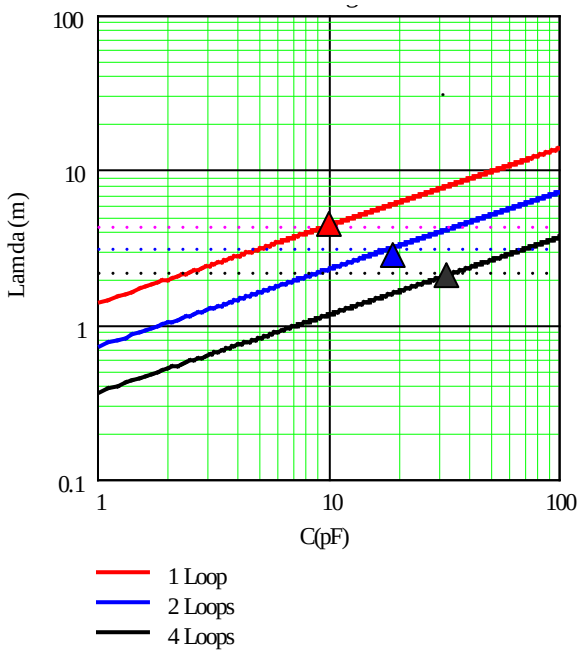

Figure 7. Plot of the wavelength of EM signals produced by the loop currents as a function of the capacitance. (The triangles indicate the limits of the low-frequency current approximation, where the sub-loop perimeter is equal to λ/2. Values of capacitance lower than those indicated on the x-axis provide resonant frequencies that are too high for the quasi-static current distribution to be valid.)

The upper frequencies for this quasi-static analysis are as follows:

Table 2.Upper frequency limits of the quasi-static loop analysis.

N =1 Loop	N = 2 Loops	N = 4 Loops
71 MHz	100 MHz	143 MHz

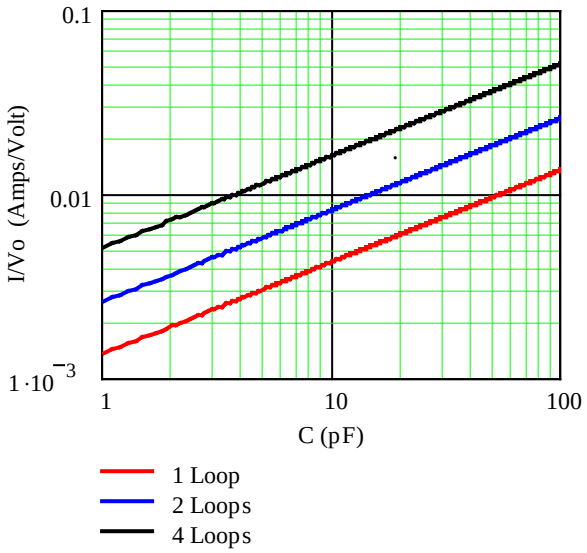

Figure 8. Plot of the normalized peak source current I_s/V_o in the circuit of Figure 5, as a function of the source capacitance, shown for different numbers of sub-loops

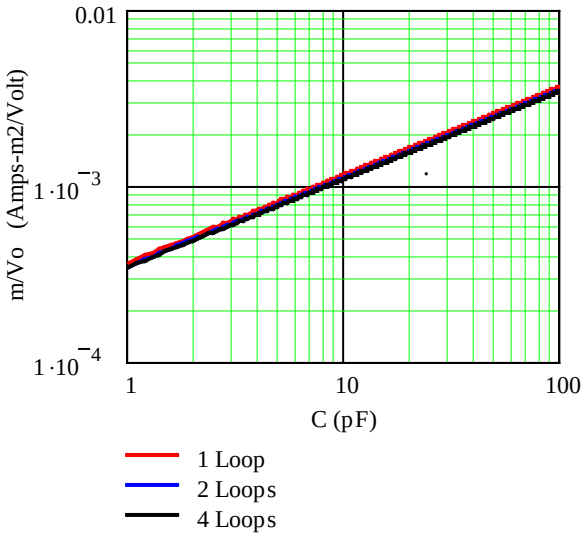

Figure 9. Plot of the normalized peak dipole moment m/V_o of the loop antenna, shown as a function of the source capacitance for different numbers of sub-loops

3. Evaluation of the Radiated EM Field

3.1 Evaluation of the Radiated E and H fields

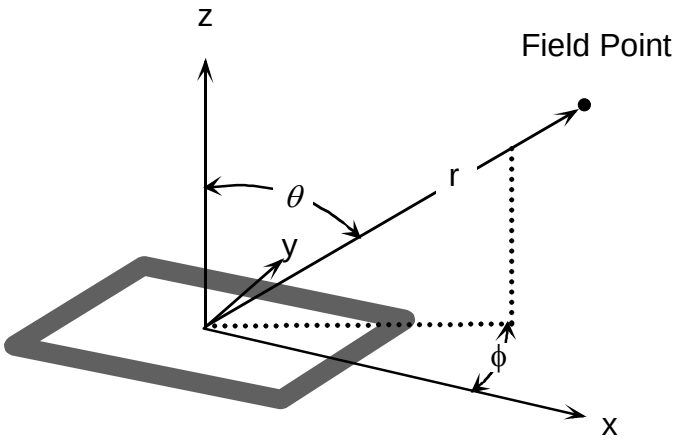

Figure 10. Illustration of the loop antenna and the spherical coordinate system for computing the radiated EM field

$$E_\phi = \frac{-j\omega\mu}{4\pi} m_z(\omega) k^2 \sin(\theta) \left[\frac{j}{kr} + \frac{1}{(kr)^2} \right] e^{-jkr} \tag{16a}$$

$$Z_o H_r = \frac{j\omega\mu}{2\pi} m_z(\omega) k^2 \cos(\theta) \left[\frac{-j}{(kr)^3} + \frac{1}{(kr)^2} \right] e^{-jkr} \tag{16b}$$

$$Z_o H_\theta = \frac{j\omega\mu}{4\pi} m_z(\omega) k^2 \sin(\theta) \left[\frac{-j}{(kr)^3} + \frac{1}{(kr)^2} + \frac{j}{kr} \right] e^{-jkr} \tag{16c}$$

In the far field, where the $[1/(kr)^2]$ and $[1/(kr)^3]$ terms are negligible, it is seen that the field is proportional to $(j\omega)^2$. This means first of all, the far field is the second time derivative of the magnetic dipole moment. Secondly, the far field is proportional to the (resonant frequency)^2, meaning the subdivision of the loop (N = 4), yields approximately N^2 (=16) times more field. This is a significant advantage gained by subdividing the loop.

To compute the radiated field, we first take a magnetic dipole moment represented by an oscillating waveform having a finite pulse width. This waveform starts at t = 5 ns and lasts until 40 ns, where the sinusoidal waveform is truncated.

This waveform has discontinuous derivatives at each end (unphysical). The terms in the radiated fields that behave as jω correspond to taking derivatives in the time domain and this yields impulse functions in the transient fields.

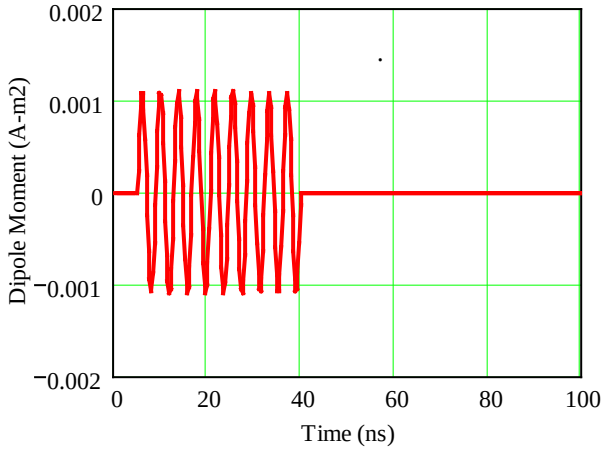

Figure 11. Transient behavior of the normalized dipole moment $m(t)/V_o$ for the pulser firing at $t = t_1 = 5$ ns. (Waveform is for C = 10 pf and N = 4 loops. The oscillating waveform is terminated at $t = 40$ ns.)

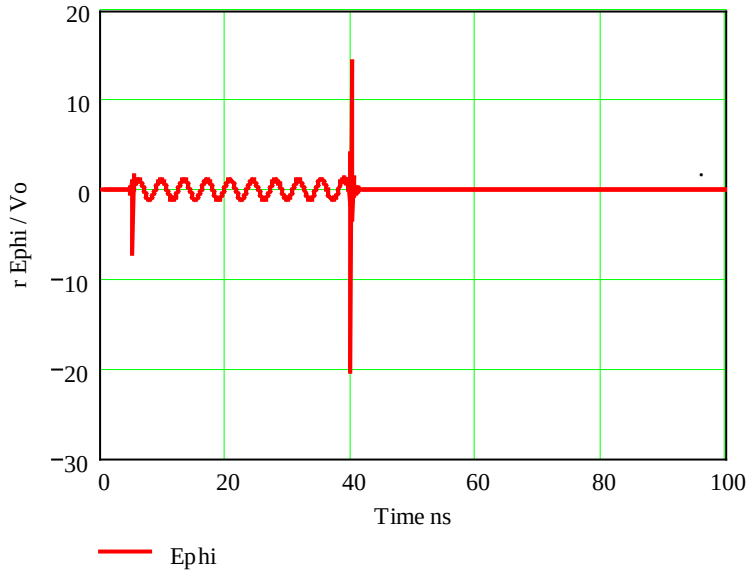

Figure 12. Plot of the normalized radiated E-field rE_ϕ/V_o produced by the transient dipole moment shown in Figure 11. (The impulses in the field at the beginning and end of the waveform are due to derivative discontinuities in the dipole moment.)

3.2 Addition of Loss to the Pulser Circuit

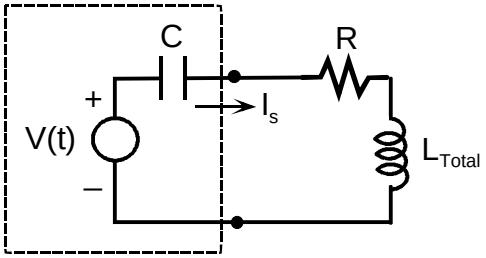

Figure 13. The pulser circuit with resistance added

We add loss to the circuit to damp the waveform, and add a finite rise. The loss is assumed to be in the pulser source, so the element R is assumed to be independent of the loop subdivisions.

Step function response

$$\begin{aligned} I_s(s) &= \left(V_o / s\right)\left(\frac{s / L_{Total}}{s^2 + sR / L_{Total} + 1/(L_{Total}C)}\right) \\ &= \left(\frac{V / L}{(s - s_1)(s - s_2)}\right) \end{aligned} \tag{17}$$

$$s_1, s_2 = -\frac{R}{2L_{Total}} \pm j\sqrt{\frac{1}{L_{Total}C} - \left(\frac{R}{2L_{Total}}\right)^2} \tag{18}$$

$$I_s(t) = \frac{V_o / L_{Total}}{\sqrt{\frac{1}{L_{Total}C} - \left(\frac{R}{2L_{Total}}\right)^2}} \sin\left(\sqrt{\frac{1}{L_{Total}C} - \left(\frac{R}{2L_{Total}}\right)^2}\,(t - t_1)\right) e^{-(R/2L_{Total})(t - t_1)}\, U(t - t_1) \tag{19}$$

$$I_s(t) \approx V_o\sqrt{\frac{C}{L_{Total}}} \sin\left(\sqrt{\frac{1}{L_{Total}C}}(t - t_1)\right) e^{-(R/2L_{Total})(t - t_1)}\, U(t - t_1) \tag{20}$$

When the large loop is subdivided into N sub-loops (see Eq.(10) the sub loop current is given as

$$I_{sub-loop}(t) \approx V_o\sqrt{\frac{C}{L_{Loop}}} \sin\left(N\omega_o(t - t_1)\right) e^{-\left(N^2R/2L_{Loop}\right)(t - t_1)}\, U(t - t_1) \tag{21}$$

Compare this equation with Eq.(12)

The total magnetic dipole moment of Eq.(15) for the lossless circuit thus becomes

$$m_{Total}(t) = V_o A \sqrt{\frac{C}{L_{Loop}}} \sin\left(N\omega_o(t-t_1)\right) e^{-\left(N^2R/2L_{Loop}\right)(t-t_1)} U(t-t_1) \qquad (22)$$

This waveform damps out exponentially at late times, and does not have a discontinuous derivative there. However, it still has a discontinuous derivative at t = t1. This can be eliminating by multiplying the transient expression in Eq.(above) by the function

$$g(t) = \frac{1}{1+e^{-\alpha(t-5t_1)}} \qquad (23)$$

Here, this function is centered at t = 25 ns and with the parameter $\alpha = 0.5 \times 10^9$, it has a width of roughly 20 ns, as shown in Figure 14

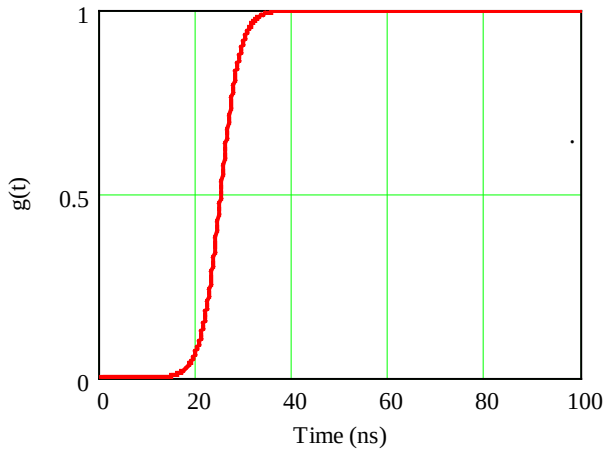

Figure 14. Plot of the function g(t) designed to modify the leading edge of the transient waveform of Figure 11

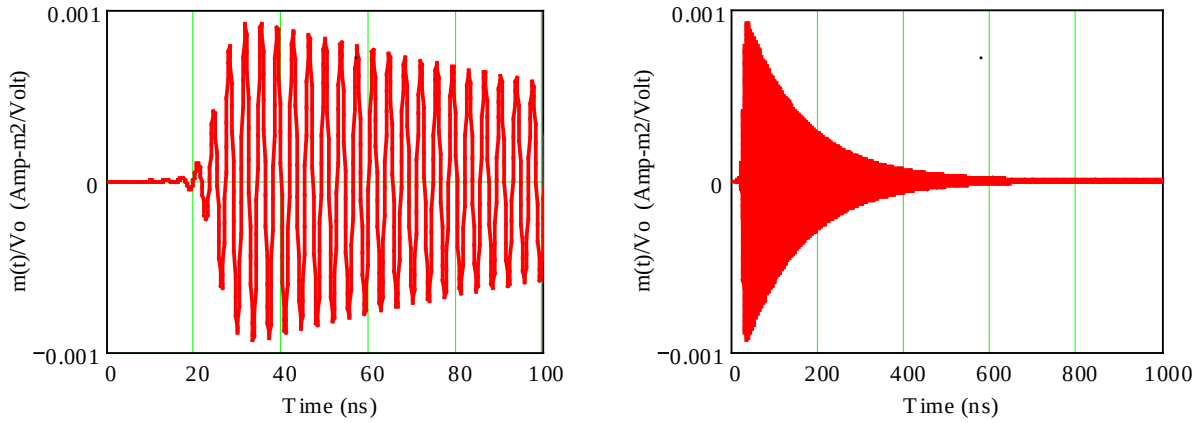

a) Early Time b) Late Time

Figure 15. Plots of the early time and late time behavior of the dipole moment of the loop antenna for *C* = 10 pf, *R* = 0.5 Ω and *N* = 4 loops.

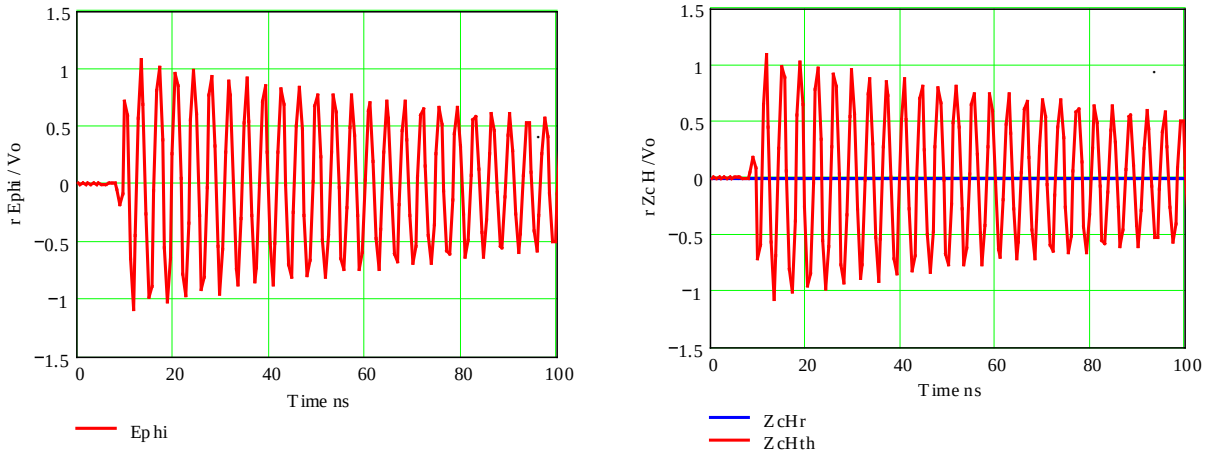

a) Normalized rE_ϕ/V_o b) Normalized rZ_cH_r/V_o and rZ_cH_θ/V_o

Figure 16. Plots of the radiated transient *E* and *H*-field components in the θ = 90º direction from the loop antenna for *C* = 10 pf, *R* = 0.5 Ω and *N* = 4 loops

NOTE:

1) These are for an assumed set of pulser capacitance, and resistance in the circuit.

2) ***We are not likely to get such a high Q in practice, since the losses in the circuit are unknown, and the radiation resistance of the loop is not included***.

4. Summary of Radiated Field Characteristics

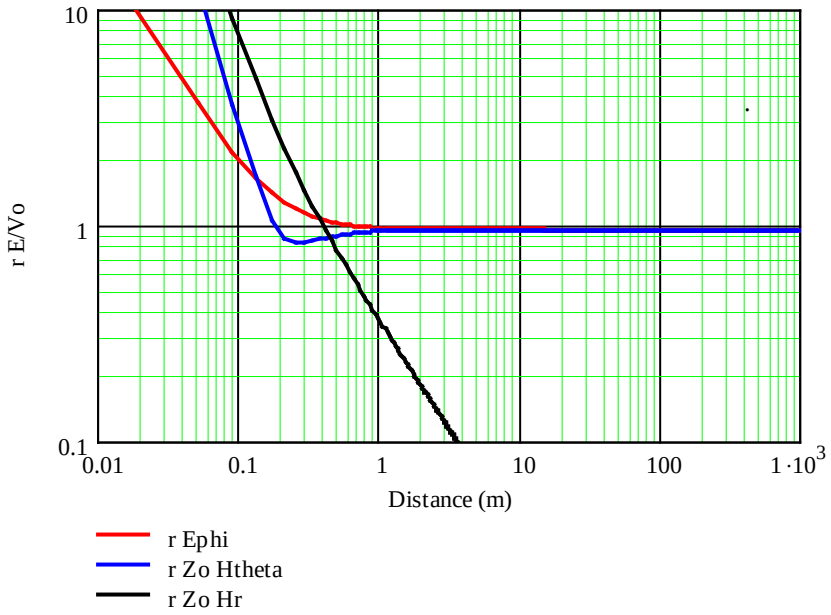

Figure 17. Behavior of the of normalized peak radiated E- and H-field components shown as a function of range for from the loop antenna for C = 10 pf, R = 0.5 Ω and N = 4 loops. The resulting frequency of oscillation of f_o = 259 MHz

NOTE:

1) It is seen that the radial component of the magnetic field goes to zero, as a function of distance, very rapidly.

2) The far field conditions of (kr ~ 1) and r > loop size at a frequency = 259 MHz are satisfied for a range of ~ 1m, which is consistent with the above plots.

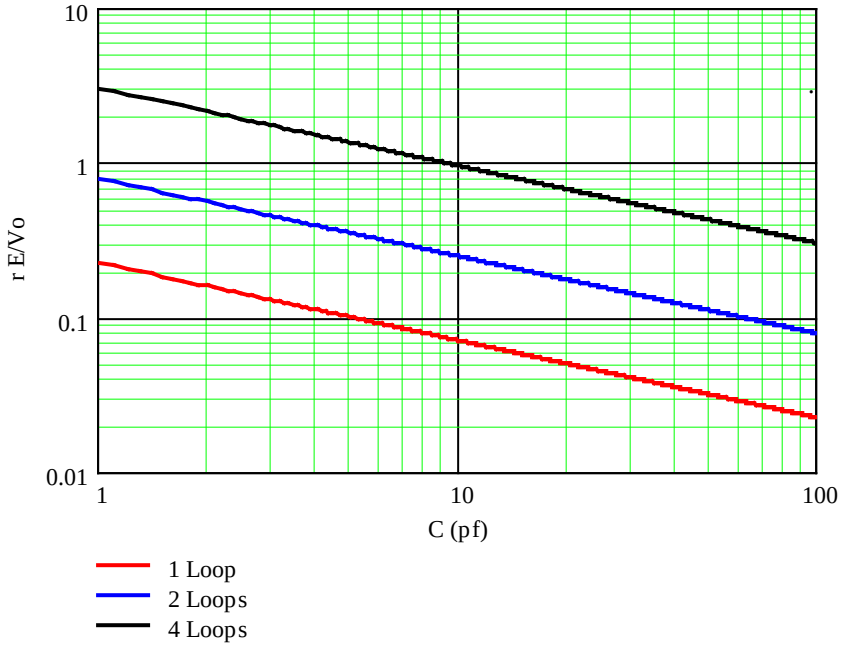

Figure 18. Plots of the peak normalized far-zone E-field rE_ϕ/V_o as a function of pulser capacitance for different numbers of sub-loops

Observe that the radiated E-field for the 4-loop case is a factor of 14 higher than the field for the single loop. Because the frequency of the radiated field is proportional to f^2, one would expect that the proportionality factor would be 16. The reason that it is slightly smaller is that the inductance of the smaller loop (as calculated from Eq(6) is not exactly ¼ that of the large single loop. This accounts for the slightly different dipole moment curves in Figure 9.

For the same reasons, the radiated field for the case of N= 2, is 3.57 times larger than the field for a single loop. It is not quite 4 times, since the frequency is not exactly 2 times, but a little less, more like 1.88 times.

5. High Frequency Models Using NEC

The previous discussion has involved a quasi-static model for determining the antenna currents and the radiated fields. For frequencies over about 100 MHz, the electrical size of the loop antenna begins to become comparable to a wavelength, and the quasi-static model becomes inaccurate. To conduct an analysis in at frequencies over 100 MHz, we can use the Numerical Electromagnetics Code (NEC) [9], which provides a numerical solution to an integral equation for the current flowing on the antenna.

The NEC code solves for currents on wire structures, and there is a limitation as to the thickness of the wire that can be accommodated in the analysis. In the present case, the effective wire radius is on the order of 7.5 cm, and for wire lengths of 60 or 45 cm the cylindrical wire is too "fat" for the NEC analysis to be accurate. Thus, NEC cannot be used to analyze the fat conductor configuration. It is possible however, to accurately treat a wire with a radius of 1 cm or smaller, and this case is reported in this section.

While NEC can model the currents on the loops better, it can not handle the wide plates, resulting in an equivalent fat, but round conductor. It still is instructive to run the NEC for a thin wire situation, although we will not be using a thin wire to make the loops. Thinner the wire, higher the inductance and lower is the resonant frequency.

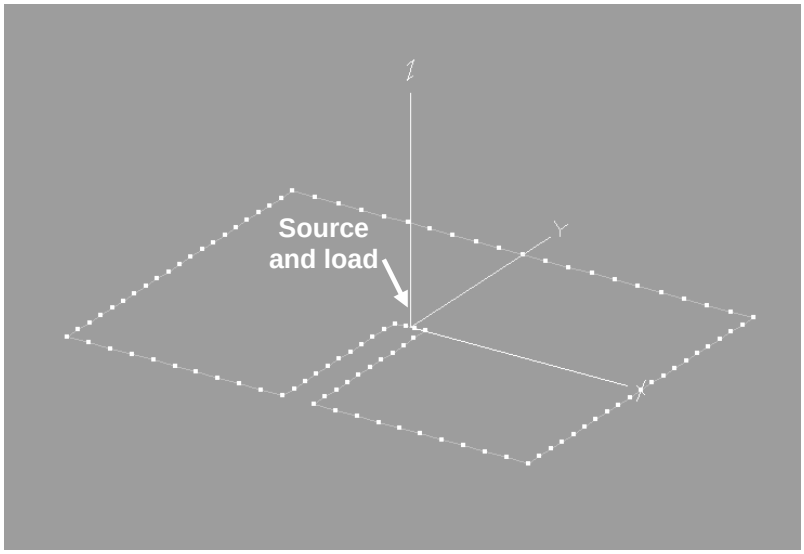

Figure 19. Illustration of the NEC model for the single loop antenna, fed by a capacitive voltage source by a transmission line

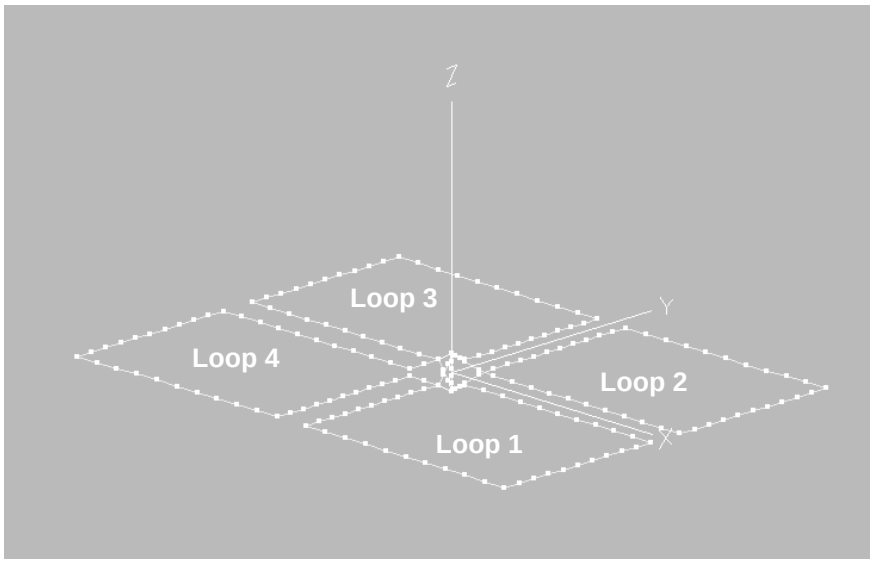

a. Overall geometry

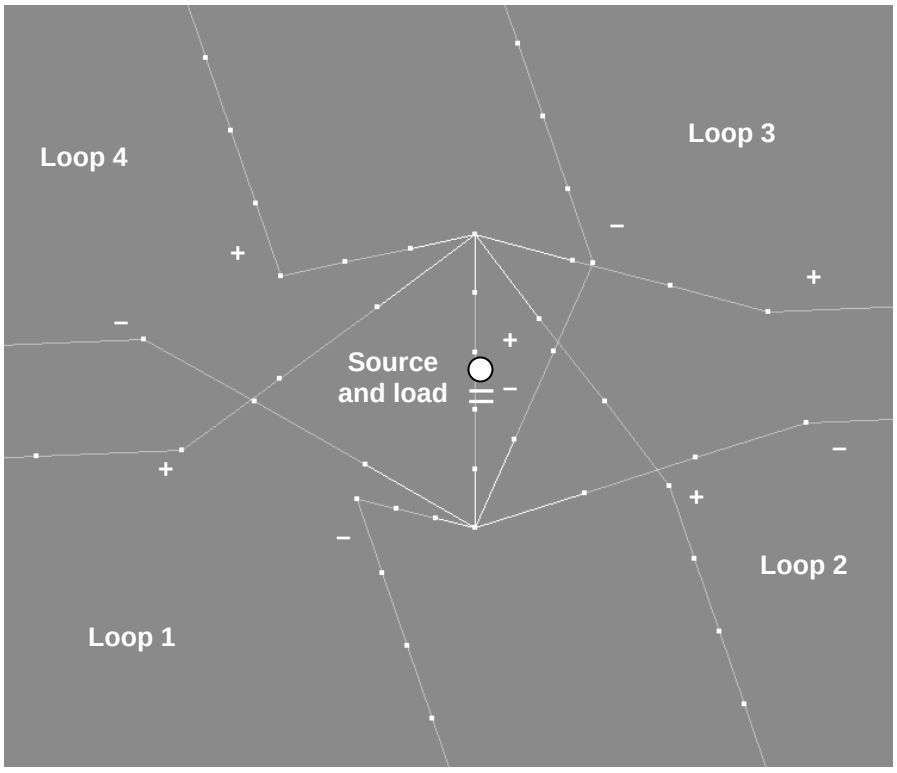

b. Source feed details

Figure 20. Illustration of the NEC model for the four loop antenna, fed by a single capacitive voltage source and four transmission lines connecting the loops in parallel

The following plot is the normalized source current (the input admittance) of the simple loop with a single source as depicted in Figure 19, with no capacitive loading of the source. The source is located at the end of the transmission line feed, as shown in the figure. Note that at low frequencies, the input current is inductive, and that the first resonance of the loop occurs at about 143 MHz, where the loop circumference is one wavelength.

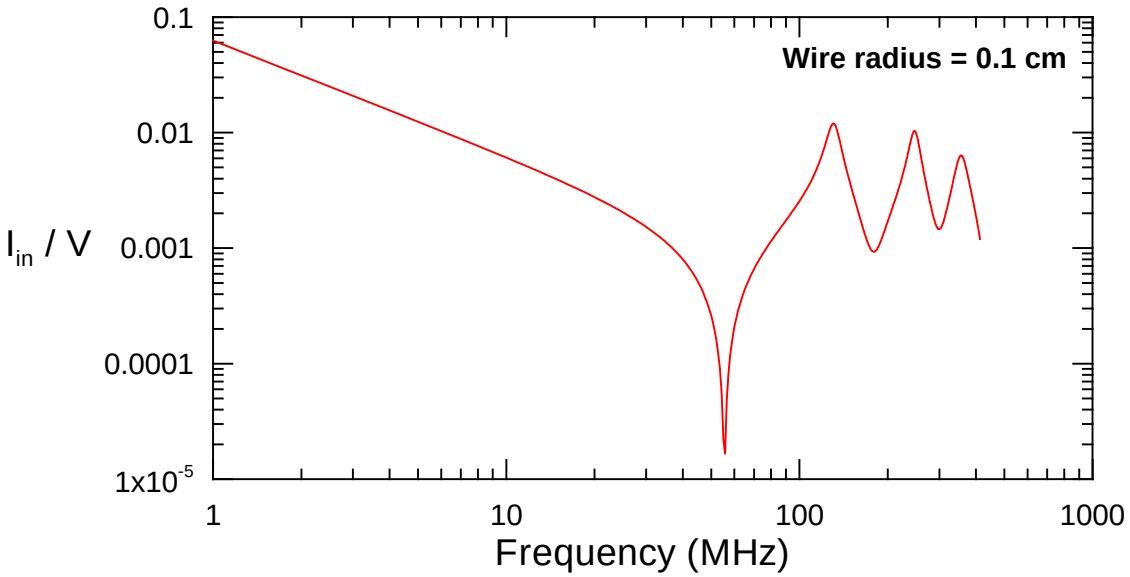

Figure 21. Plot of the computed input admittance of the loop shown in Figure 19 (with no capacitive loading)

The normalized radiated E-field (rE/V) can be computed by NEC. With reference to Figure 10, the E_ϕ field component dominates, and this is plotted in Figure 22 for the case $\theta = 90^o$ and $\phi \approx 0^o$. Note that the largest resonance occurs at f ≈ 286 MHz, which is the second current resonance. At the frequency of the first current resonance, there is a corresponding peak in the radiated field, but it is relatively small.

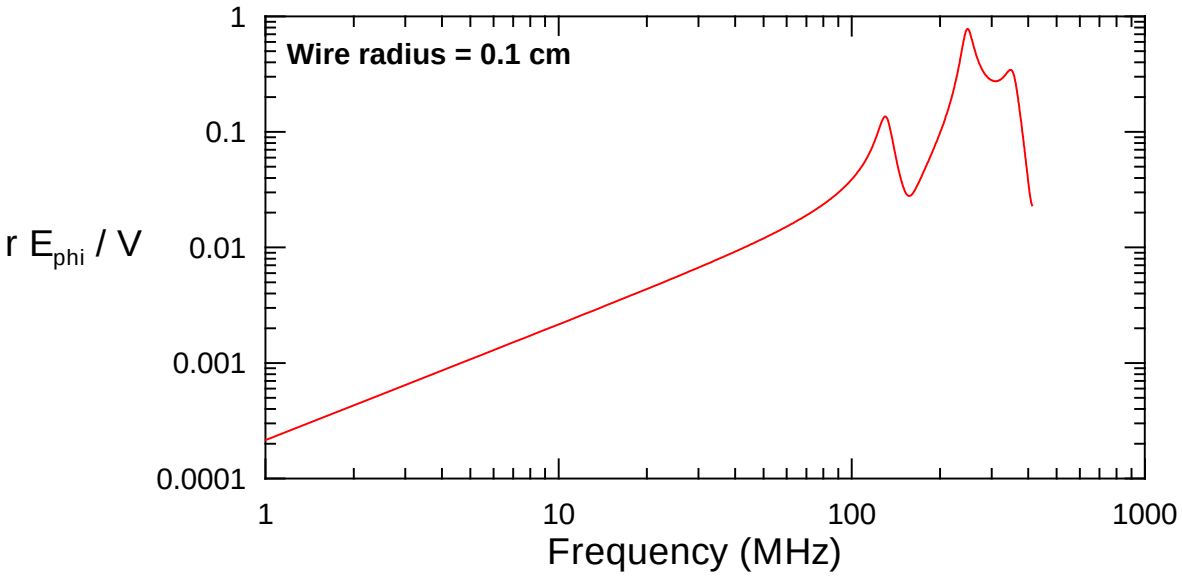

Figure 22. Plot of the normalized radiated E-field magnitude $|r\ E_\phi/V|$ for the loop of Figure 19 (with no capacitive loading)

We now add a 10 pF capacitive load at the source location on one of the wires of the loop. Figure 23 shows the effect on the input admittance: a L-C circuit resonance has been introduced at low frequencies. Using the inductance of the loop as given by Eq.(6), these resonances are calculated to be 43.5 MHz for the 1 cm wire. These frequencies agree with the resonances in Figure 23. Note that at these frequencies, the loop still is electrically small. The resonances are not due to the resonant behavior of current on the loop structure, but rather, they are due to the interaction of the loop inductance and the source capacitance.

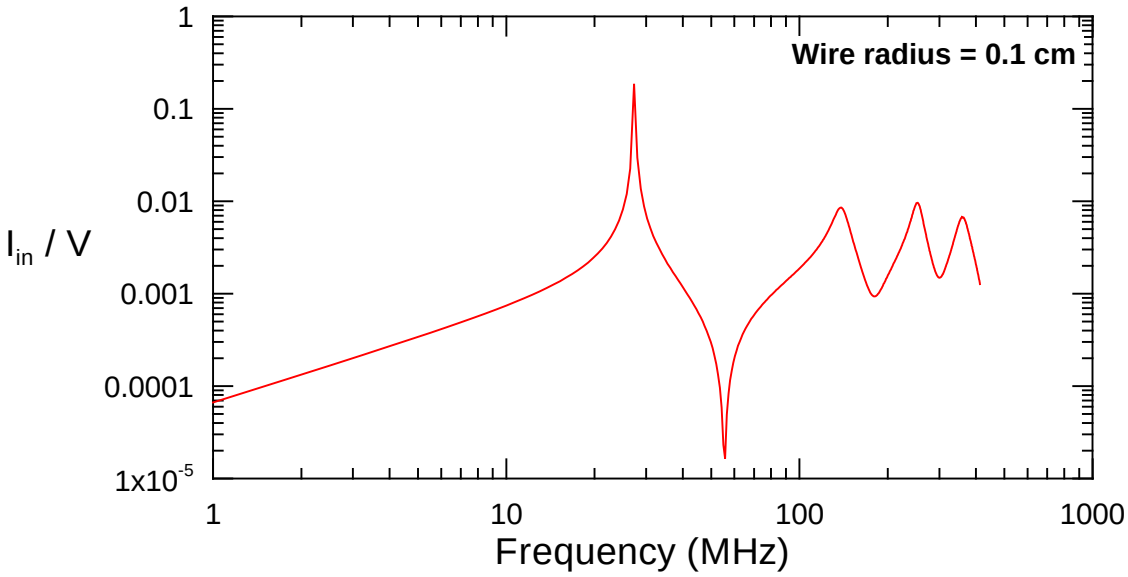

Figure 23. Plot of the input admittance of source of Figure 19 with 10 pF capacitive load at a single source

Figure 24 presents the radiated E-field magnitude $|r\ E_{phi}/V|$ from loop in the direction $\theta = 90^o$ and $\phi = 0^o$. for the single excitation source with a capacitive load of 10 pF.

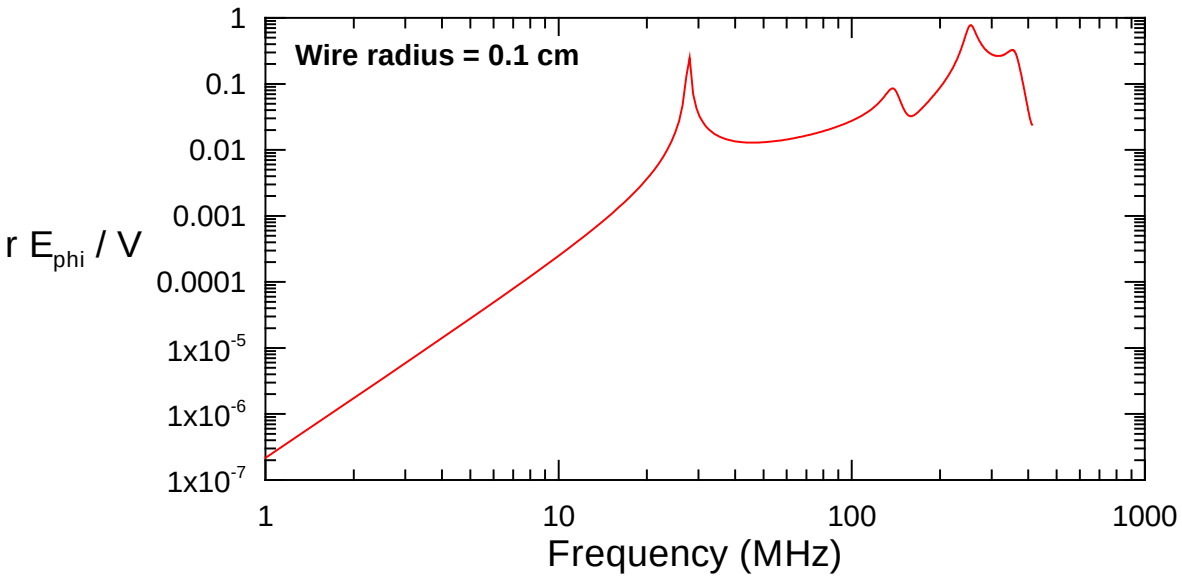

Figure 24. Plot of the normalized radiated E-field magnitude $|r\ E_{\phi}/V|$ from loop of Figure 19 with 10 pF capacitive load at a single source.

Next, we divide the loop into four separate loops, as shown in Figure 20. This is done by modeling the transmission lines by two parallel conductors, which connected in parallel to the voltage source with capacitive source impedance.

The resulting radiation pattern for this case is shown in Figure 25. Note that the effect of subdividing the single loop is to raise the L-C resonance by a factor of about 3.2. This is not exactly equal to the factor of 4 increase in frequency predicted by the low frequency model. Note also that the peak amplitude of the L-C resonance of the four-loop case is about 16 times larger than that for the single loop due to the f^2 dependence of the radiated field.

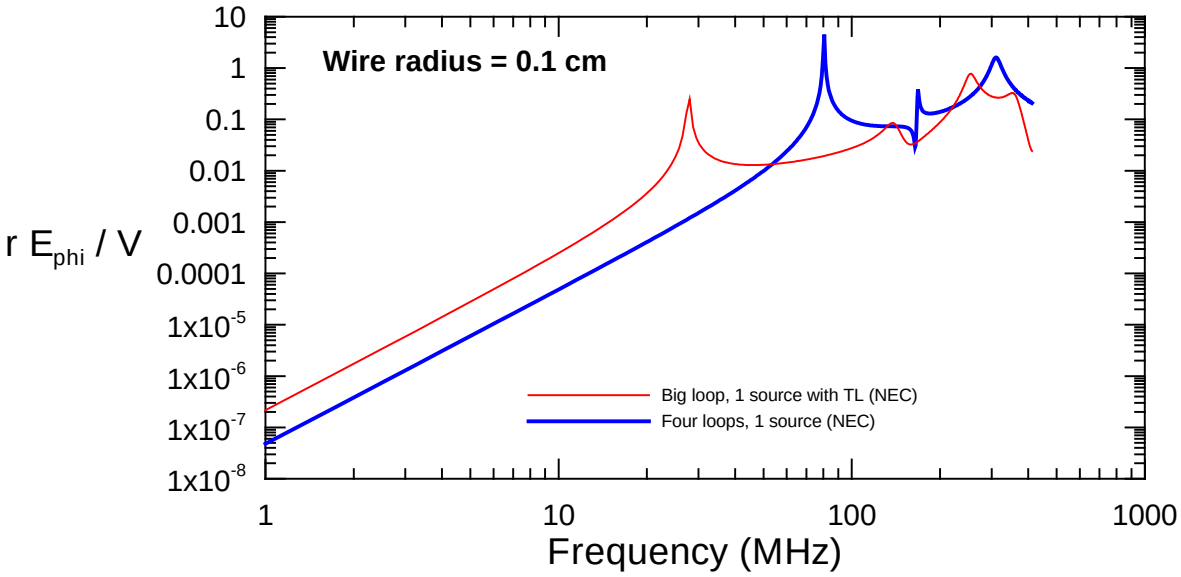

Figure 25. Plots of the radiated E-field magnitude $|r\ E_\phi/V|$ from the loop with 1 and 4 capacitive (10 pF) voltage sources in the direction θ = 90º and ϕ = 0º.

It is instructive to examine the behavior of the radiation pattern around the 4-loop antenna. With reference to the coordinate system shown in Figure 10, calculations of the normalized principal field component $|r\ E_\phi/V|$ in the z = 0 plane (for θ = 90º) have been computed for azimuthal angles ϕ = 0º, 30º, 60º and 90º. These spectral plots are shown in Figure 26. Note that for frequencies lower than about 110 MHz, the radiation pattern is omni directional. However, above this frequency, there is a noticeable variation of the pattern with the angle ϕ.

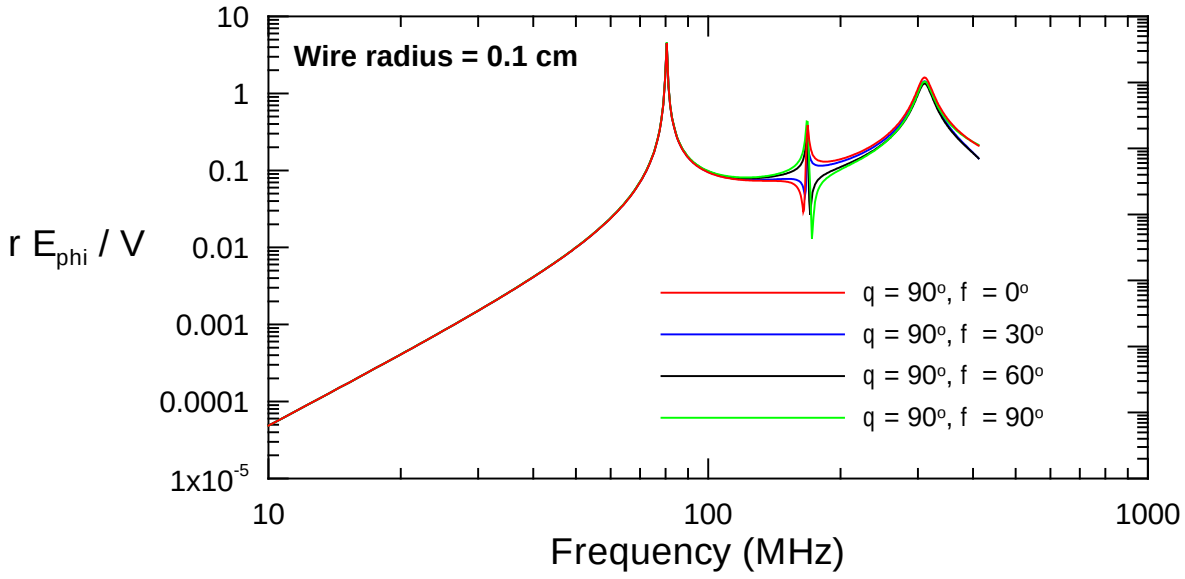

Figure 26. Behavior of the normalized radiated E-field magnitude $|r\ E_{phi}/V|$ for an observation location on the z = 0 plane ($\theta = 90^{\circ}$) for different values of the azimuth

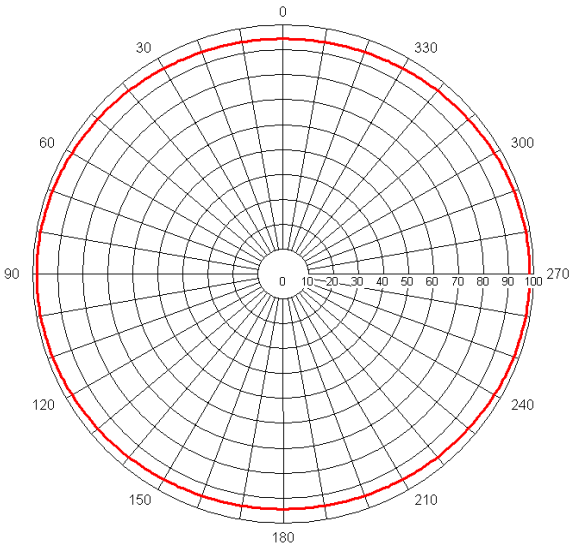

a. Frequency = 100 MHz

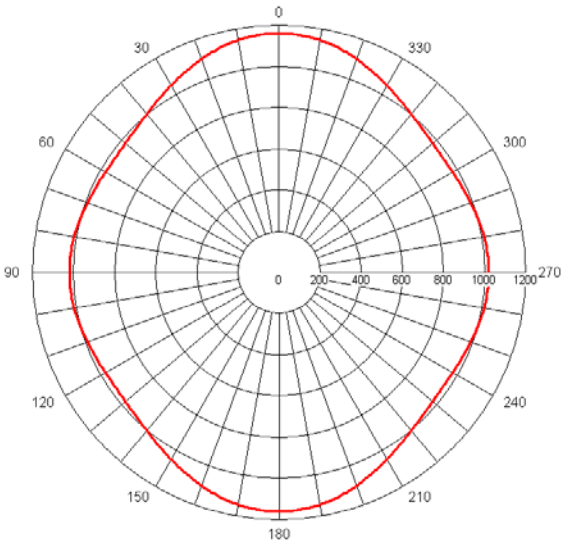

b. Frequency = 300 MHz

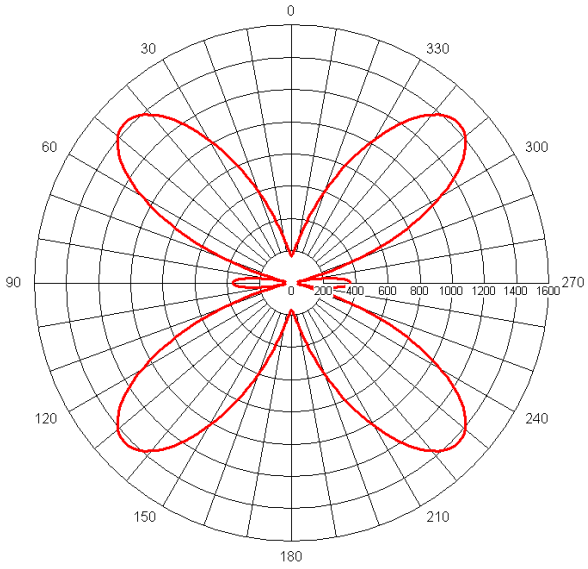

c. Frequency = 600 MHz

Figure 27. Plots of the normalized radiation pattern $|r\,E_{phi}/V|$ in the horizontal plane ($\theta = 90^{o}$) for three different frequencies. (The radial scale is x 10^3, so that the quantity being plotted in units of [meters] x [millivolts/meter] / [volts].)

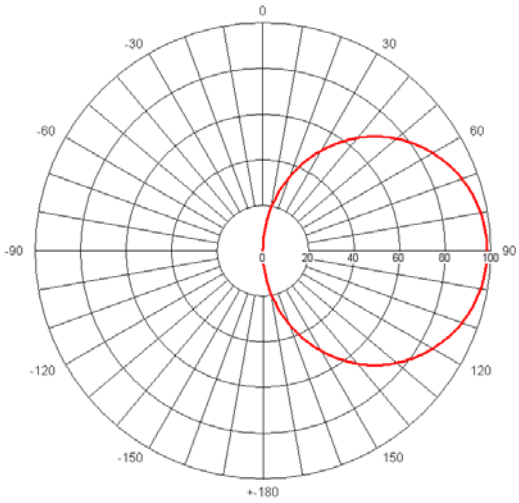

a. Frequency = 100 MHz

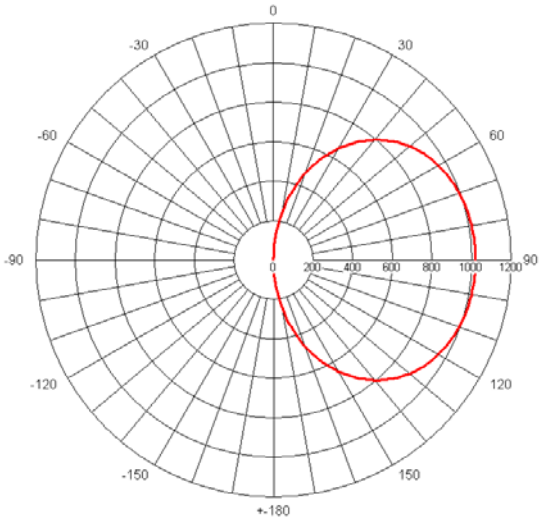

b. Frequency = 300 MHz

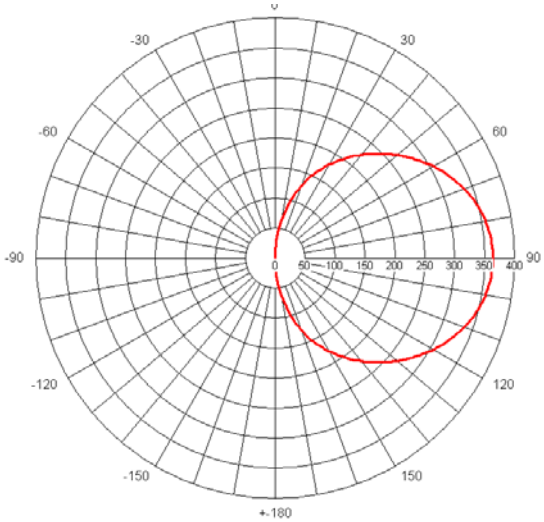

c. Frequency = 600 MHz

Figure 28. Plots of the normalized radiation pattern $|r\ E_{phi}/V|$ in the vertical plane (ϕ = 90$^{o)}$ for three different frequencies. (The radial scale is x 10^3, so that the quantity being plotted in units of [meters] x [millivolts/meter] / [volts].)

Next, we consider an electrical dipole for comparison, as shown in figure 29.

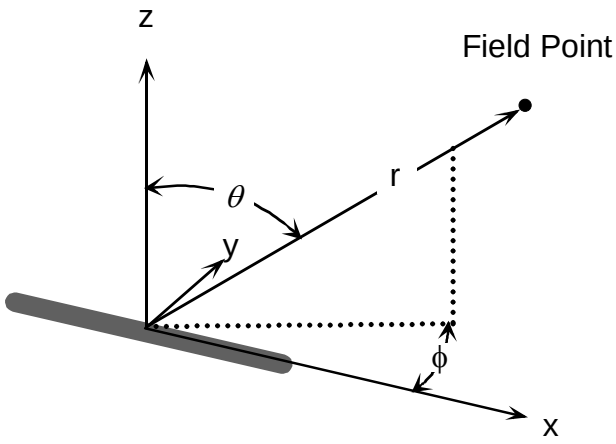

Figure 29. Illustration of a thin rod antenna and the spherical coordinate system for computing the radiated field

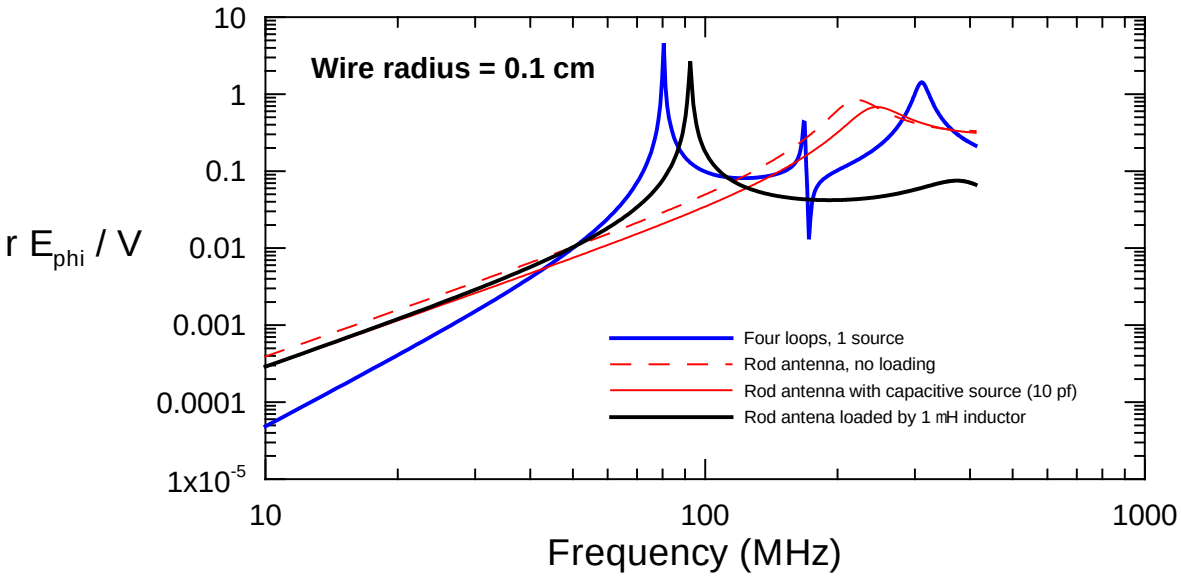

Figure 30. Plot of the radiated normalized E-field $|r\ E_{phi}/V|$ for the observation angles $\theta = 90^o$, $\phi = 90^o$ for the rod and 4-loop antennas

It is noted that the 4 loops (N = 4) driven in parallel by one capacitive source that maximizes the magnetic dipole moment is still the preferred choice for the antenna.

Shown below are plots of the radiated E-field for the observation angles $\theta = 90^o$, $\phi = 90^o$ for different wire radii. Note that as the wire's thickness increases, so does the L-C resonant frequency. AS the wire thickness increases, the inductance decreases thus, increasing the resonant frequency. Thus, in the original concept of the wide plate antenna, the resonant frequency is maximized for the space allowed for the antenna.

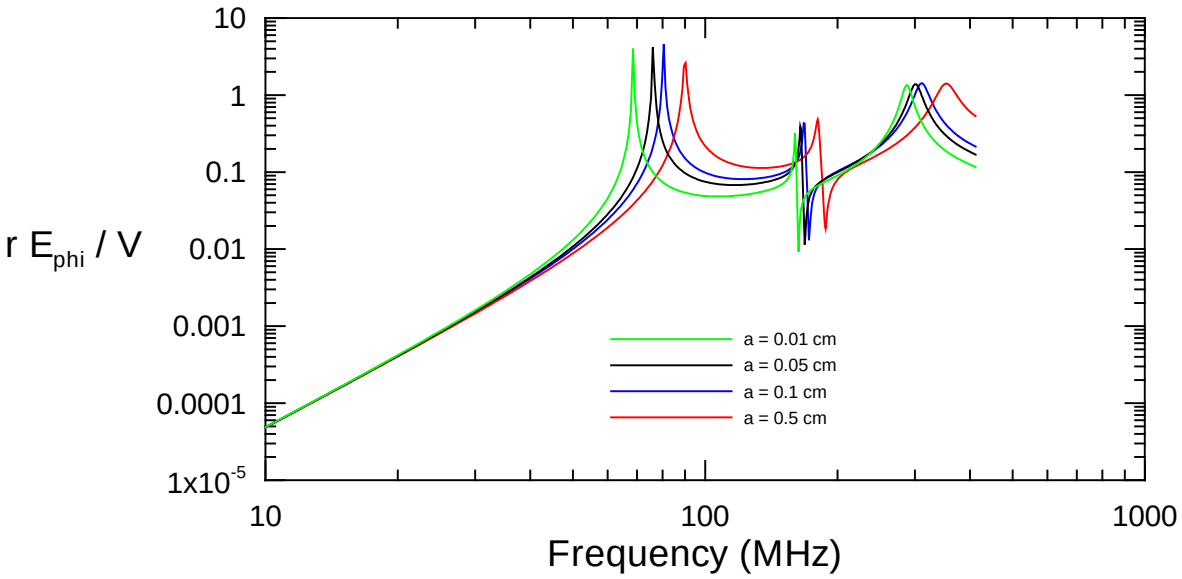

Figure 31. Illustration of the sensitivity of the 4-loop radiated field for variations of the wire radius

6. Summary Comments

We have addressed the design considerations of a magnetic dipole or a loop antenna for a capacitive compact source. Baum's suggestion of subdividing the loop into N parts has been shown to lead to many advantages. The subdivision into N loops (N = 4) is a good choice leading to:

- Setting up a circuit or LC type of resonance between the source capacitance and the loop inductance; this resonance is at a lower frequency than the loop resonance
- Approximately decreases the value of the total inductance by a factor of N^2
- Approximately increases the resonant frequency by a factor of N
- The total magnetic moment of the subdivided loop is the same as the magnetic moment of the single loop

- However, since the far field from a magnetic dipole is proportional to the square of the frequency, the far field increases approximately by a factor of N^2

- The resistive losses in the circuit leads to an exponential damping term that has N^2 in the exponent; this suggests that subdivision can not be carried too far

- For the case of N = 4, and utilizing the prescribed maximum dimensions, we find the loop inductance is about 33 nH and it is likely that the Marx inductance may turn out to be a factor of 4 or 5 more than this value and the source capacitance and inductance may ultimately determine the resonant frequency.

- Some of the calculations in this note are for assumed parameters of source capacitance of 10 pF, N = 4, utilize some typical dimensions and for a resistance in the circuit of 0.5 Ohms. We are not likely to obtain the high Q values estimated in this note, because of radiation resistance and the losses in the circuit which are not precisely known.

- Subdividing the original single loop into 4 loops will increase the required volume somewhat, since interconnections between the sub-loops become necessary. We have considered a loop antenna in this note, because the source is capacitive and the inductance of the loop antenna can be exploited for an LC resonance. If we build a single loop antenna with a Marx source, we have shown that subdividing the loop into 4 loops is beneficial, without significantly increasing the needed volume.

References

1. G. Staines, “Compact Sources for Tactical RF Weapon Applications”, presented at AMEREM 2002, U. S. Naval Academy, Annapolis, MD, June 2002

2. D. K. Chang, **Analysis of Linear Systems,** Addison-Wesley, Reading, Mass., 1959.

3. F. W. Grover, **Inductance Calculations: Working Formulas and Tables**, D. Van Nostrand Company, New York, 1946.

4. F. E. Terman, **Radio Engineers' Handbook**, London, McGraw-Hill, 1st ed., Sep. 1950.

5. V. I. Bashenoff, “Supplementary Note to Abbreviated Method for Calculating the Inductance of Irregular Plane Polygons of Round Wire,” Proc. IRE, vol. 16, no. 11, pp. 1553-1558, Nov. 1928.

6. C. R. Paul, **Introduction to Electromagnetic Compatibility**, John Wiley and Sons, New York, 1992.

7. C. E. Baum, Private Communication, March-April 2005.

8. C. E. Baum, “Compact, Low-Impedance Magnetic Antennas’, Sensor and Simulation Note 470, December 2002.

9. Numerical Electromagnetics Code – NEC Point of contact: Jerry Burke, Lawrence Livermore National Laboratory, P.O. Box 808, Livermore, CA 94550, (510) 422-1100